Eur. J. Mineral.
2017, **29**, 1031–1044
Published online 26 June 2017

Claraite, $(Cu,Zn)_{15}(AsO_4)_2(CO_3)_4(SO_4)(OH)_{14}\cdot 7H_2O$: redefinition and crystal structure

CRISTIAN BIAGIONI* and PAOLO ORLANDI

Dipartimento di Scienze della Terra, Università di Pisa, Via S. Maria 53, 56126 Pisa, Italy
*Corresponding author, e-mail: cristian.biagioni@unipi.it

Abstract: Since the beginning of the 2000s, several authors reported the occurrence of As and S as chemical components of the hydrated copper hydroxy-carbonate claraite, originally described with the formula $(Cu,Zn)_3(CO_3)(OH)_4\cdot 4H_2O$. Owing to the lack of knowledge about the crystal structure of this mineral, the structural role played by these chemical elements was unknown. The crystal structure of claraite has now been solved from single-crystal X-ray diffraction data by using a specimen from the marble quarries of Carrara, Apuan Alps, Tuscany, Italy. Electron-microprobe analyses gave (in wt% – average of eight spot analyses): SO_3 4.00, As_2O_5 13.16, CuO 52.64, ZnO 9.03, $CO_{2(calc)}$ 9.08, $H_2O_{(calc)}$ 12.56, total 100.47. On the basis of 15 (Cu + Zn) and 45 O atoms per formula unit, the chemical formula of claraite could be written as $(Cu_{12.85}Zn_{2.15})_{\Sigma 15.00}(AsO_4)_{2.22}(CO_3)_4(SO_4)_{0.97}(OH)_{13.40}\cdot 6.83H_2O$, ideally $(Cu,Zn)_{15}(AsO_4)_2(CO_3)_4(SO_4)(OH)_{14}\cdot 7H_2O$. Raman spectrometry shows bands related to bending and stretching vibrations of AsO_4 and SO_4 groups, as well as the stretching mode of CO_3 groups and O–H bonds. The unit-cell parameters of claraite are $a = 10.3343(6)$ Å, $b = 12.8212(7)$ Å, $c = 14.7889(9)$ Å, $\alpha = 113.196(4)°$, $\beta = 90.811(4)°$, $\gamma = 89.818(4)°$, $V = 1800.9(2)$ Å^3, space group $P\bar{1}$. The crystal structure has been refined to $R_1 = 0.111$ on the basis of 6956 reflections with $F_o > 4\sigma(F_o)$ and 363 refined parameters. Claraite shows a layered structure, with {0 0 1} heteropolyhedral layers formed by $Cu\phi_5$ and $Cu\phi_6$ polyhedra as well as AsO_4 and CO_3 groups. These layers are stacked along **c** through edge-sharing $Cu_2\phi_{10}$ and $Cu_2\phi_8$ dimers, the former being decorated by corner-sharing SO_4 groups hosted within intra-framework channels together with H_2O groups. Claraite is the only known mineral showing the simultaneous occurrence of essential AsO_4, CO_3, and SO_4 groups.

Key-words: claraite; crystal structure; Raman spectroscopy; carbonate; sulfate; arsenate; copper; Carrara; Apuan Alps.

1. Introduction

Claraite is a relatively rare secondary copper mineral, originally described by Walenta & Dunn (1982) from the Clara mine, central Black Forest, Baden-Württemberg, Germany, in association with malachite, azurite, and olivenite. The ideal chemical composition was given as $(Cu,Zn)_3(CO_3)(OH)_4\cdot 4H_2O$. Owing to the lack of samples suitable for single-crystal study, only the X-ray powder diffraction pattern was reported; it was indexed on the basis of a hexagonal pseudocell, even if the authors hypothesized a triclinic symmetry on the basis of the optical properties. Later, Walenta (1999) reported a new indexing of the X-ray powder diffraction pattern of claraite on the basis of a triclinic cell, with $a = 14.28$ Å, $b = 8.03$ Å, $c = 7.27$ Å, $\alpha = 79.16°$, $\beta = 107.90°$, $\gamma = 99.68°$.

Since the beginning of the 2000s, new chemical data pointed to the presence of As and S as components of claraite (*e.g.*, Schnorrer, 2000; Kolitsch & Brandstätter, 2012; Putz *et al.*, 2012). However, the crystal-chemical role of these two elements remained unknown, owing to the lack of knowledge about the crystal structure. The identification of a new occurrence of claraite from the Gioia marble quarries, Carrara, Apuan Alps, Tuscany, Italy, allowed us to find crystals which, although of very low quality, were nevertheless amenable to a single-crystal X-ray diffraction study. It was then possible to solve and refine the crystal structure of claraite, highlighting the structural role of arsenic and sulfur.

The redefinition of claraite as a copper–zinc arsenate–carbonate–sulfate–hydroxide–hydrate mineral has been approved by the IMA CNMNC (proposal 16-L). This paper represents the formal redefinition of claraite and reports the description of its crystal structure.

2. Experimental procedure

2.1. Studied specimens

The finding of claraite in cavities of marble excavated in the Carrara quarries, Apuan Alps, Tuscany, Italy, was first reported by Orlandi (1999) who studied a specimen collected at La Facciata quarry. Claraite occurs as mm-sized rounded aggregates, formed by very small blue tabular crystals; its identification was based on an X-ray powder diffraction pattern collected with a Gandolfi

DOI: 10.1127/ejm/2017/0029-2669
0935-1221/17/0029-2669 $ 6.30

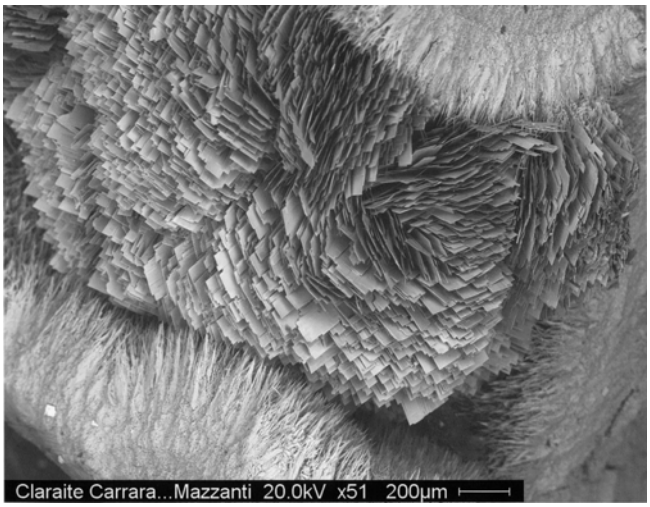

Fig. 1. Claraite, thin tabular crystals associated with an unidentified fibrous Cu–Zn chloro-arsenate–carbonate. Gioia quarries, Carrara, Apuan Alps, Tuscany, Italy. Collection Museo di Storia Naturale, University of Pisa. Catalogue number 19899.

Table 1. Electron microprobe analyses of claraite from Carrara.

Oxide	wt% ($n = 8$)	Range	σ
SO_3	4.00	3.92–4.07	0.04
As_2O_5	13.16	12.75–13.61	0.34
CuO	52.64	50.67–54.16	1.17
ZnO	9.03	8.41–9.32	0.31
CO_2*	9.08		
H_2O*	12.56		
Total	100.47		

* H_2O and CO_2 were calculated taking into account the structural formula.

camera and qualitative chemical analyses. Later, new specimens were found in the Gioia quarries, where the sample studied in this work was collected by the mineral amateur Riccardo Mazzanti. Claraite occurs as blue-green globular aggregates of thin tabular nearly rectangular crystals, up to 200 µm in length and less than 10 µm thick (Fig. 1). It is associated with a still unidentified fibrous green-colored Cu–Zn chloro-arsenate–carbonate.

In order to confirm the identity of this new occurrence with claraite from the type locality, two additional specimens from the Clara mine were examined. The first one was represented by few loose mm-sized grains showing blue-green spherules up to ~0.5 mm. These grains belong to the holotype material and were kindly provided by the Smithsonian Institution – National Museum of Natural History (catalogue number NMNH 148464). In the second one, provided by the mineral collector Vittorio Mattioli, claraite occurred as blue-green globular aggregates formed by thin tabular crystals, up to 100 µm in length and less than 5 µm in thickness, associated with fluorite, malachite, and gypsum.

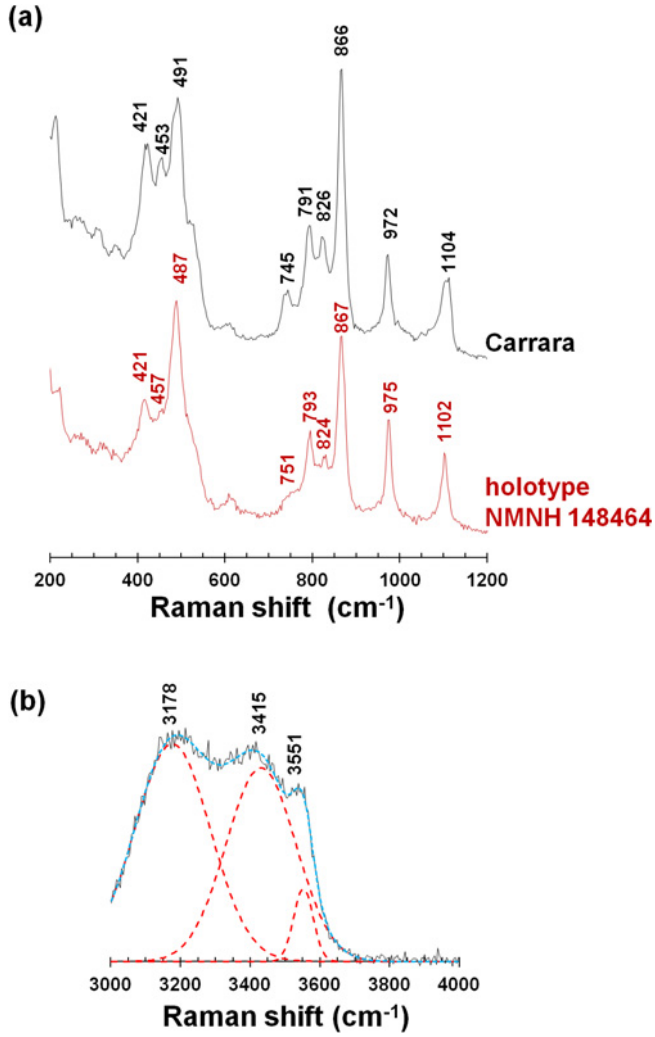

Fig. 2. Raman spectra of claraite. In (a), the region between 200 and 1200 cm^{-1} of samples from Carrara and the Clara mine (holotype specimen NMNH 148464) is shown. In (b), the region between 3000 and 4000 cm^{-1} of the sample from Carrara is shown. The Raman shift (in cm^{-1}) of the main Raman bands is reported.

2.2. Chemical data and micro-Raman spectrometry

Preliminary energy-dispersive spectrometry chemical analyses were performed on the available specimens using a Philips XL30 scanning electron microscope equipped with an EDAX DX4 detector. The spectra of all samples are practically identical in appearance, being characterized by the occurrence of Cu, Zn, As, and S as the only elements with $Z > 9$, in agreement with the chemical data reported by several authors since 2000.

Quantitative wavelength-dispersive spectrometry chemical data were collected with an ARL-SEMQ electron microprobe only on the specimen from Carrara used for the single-crystal X-ray diffraction study. The operating conditions were: accelerating voltage 15 kV, beam current 10 nA. The beam size was defocused to 20 µm in order to avoid sample damage. Counting time for

Table 2. Band positions (in cm^{-1}) and interpretation of the micro-Raman spectrum of claraite in the region between 100 and 1200 cm^{-1}.

Observed Raman band positions		Interpretation
Carrara	NMNH 148464	
215	220	Lattice vibrations
266	270	
312	322	AsO_4 and SO_4 bending modes
351	350	
392	–	
421	420	
453	457	
491	487	
523	522	
536	–	
608	612	
745	751	AsO_4 stretching modes
791	793	
826	824	
866	866	
972	975	SO_4 stretching mode
1087	1102	CO_3 and SO_4 stretching mode
1108		

each of the eight spot analyses was 10 s for peak and 5 s for background. Standards were (element, emission line): $Cu_{94}Zn_6$ (Cu*K*α), metal Zn (Zn*K*α), arsenolite (As*L*α), and baryte (S*K*α). Analytical results are given in Table 1.

The empirical formula of claraite, calculated on the basis of 15 (Cu + Zn) and 45 O atoms per formula unit (apfu), is $(Cu_{12.85}Zn_{2.15})_{\Sigma 15.00}(AsO_4)_{2.22}(CO_3)_4(SO_4)_{0.97}(OH)_{13.40}\cdot 6.83H_2O$, in agreement with that derived from the crystal structure study (see below), *i.e.* $(Cu,Zn)_{15}(AsO_4)_2(CO_3)_4(SO_4)(OH)_{14}\cdot 7H_2O$.

Unpolarized micro-Raman spectra were obtained on unpolished and randomly oriented samples of claraite from Carrara and the Clara mine in nearly back-scattered geometry with a Jobin-Yvon Horiba XploRA Plus apparatus, equipped with a motorized *x–y* stage and an Olympus BX41 microscope with a 10× objective. The Raman spectra were excited by the 532 nm light of a solid-state laser attenuated to 25%. The minimum lateral and depth resolution was set to a few μm. The system was calibrated using the 520.6 cm^{-1} Raman band of silicon before each experimental session. Spectra were collected through multiple acquisition with single counting times of 60 s. Backscattered radiation was analyzed with a 1200 mm^{-1} grating monochromator. Peak deconvolution was performed through the software *Fityk* (Wojdyr, 2010).

The Raman spectra of claraite from Carrara and the holotype material from the Clara mine are shown in Fig. 2a and the band positions (in cm^{-1}) as well as their interpretation are reported in Table 2. The Raman spectrum of claraite, in the region between 100 and 1200 cm^{-1}, can be divided into three parts:

– 100–300 cm^{-1}: this range shows bands probably related to lattice vibrations;
– 300–700 cm^{-1}: in this region, bands related to bending modes of the $(AsO_4)^{3-}$ and $(SO_4)^{2-}$ groups occur;
– 700–1200 cm^{-1}: this region includes the symmetric stretching region of $(AsO_4)^{3-}$, $(SO_4)^{2-}$, as well as $(CO_3)^{2-}$ ions. In agreement with published band assignments for the chemically related copper arsenate–sulfate parnauite (Frost *et al.*, 2009), bands ranging between 745 and 866 cm^{-1} could be attributed to the stretching of $(AsO_4)^{3-}$ groups. In particular, the bands at 866 and 826 cm^{-1} could be related to the $\nu_1(AsO_4)^{3-}$ symmetric stretching and $\nu_3(AsO_4)^{3-}$ antisymmetric stretching modes, respectively. In addition, the band at 791 cm^{-1} is also ascribed to the $\nu_3(AsO_4)^{3-}$ mode. In other arsenate-bearing minerals, the bands close to 740 cm^{-1} are attributed to hydroxyl deformation modes (*e.g.*, the band at 738 cm^{-1} in carminite and 733 cm^{-1} in kankite – Frost & Kloprogge, 2003). The sharp band at 972 cm^{-1} is attributed to the $\nu_1(SO_4)^{2-}$ symmetric stretching mode. The band at ~1104 cm^{-1} is actually formed by two components at 1108 and 1087 cm^{-1}, probably related to the $\nu_3(SO_4)^{2-}$ antisymmetric stretching mode and the $(CO_3)^{2-}$ symmetric stretching mode, respectively (*e.g.*, Frost *et al.*, 2003).

In the region between 3000 and 4000 cm^{-1}, the Raman spectrum of claraite shows a broad band (Fig. 2b); its deconvolution suggests the presence of three different bands, at ~3178, ~3415, and ~3551 cm^{-1}, attributed to the O–H stretching vibrations of the OH and H_2O groups. By using the relationships between O–H stretching frequencies and O···O distances proposed by Libowitzky (1999), the three Raman bands could correspond to three kinds of hydrogen bonds, *i.e.* short (= strong) bonds (O···O ~2.70 Å), intermediate bonds (O···O ~2.81 Å), and long (= weak) bonds (O···O ~3.00 Å).

2.3. Crystallography

X-ray powder diffraction (XRPD) patterns of claraite were collected using a 114.6 mm Gandolfi camera with Ni-filtered Cu*K*α radiation on samples from Carrara and the Clara mine. The observed patterns are reported in Table 3, where they are compared with that reported by Walenta & Dunn (1982) in the original description of claraite. In addition, the XRPD pattern calculated through the software *PowderCell* (Kraus & Nolze, 1996) on the basis of the structural model discussed below is given. Owing to the large number of indices for the majority of the diffraction lines, the unit-cell parameters of claraite were not refined from the XRPD data.

X-ray intensity data collection was performed on a small tabular crystal (150 μm × 50 μm × 10 μm in size) from Carrara, using a Bruker Smart Breeze diffractometer (50 kV, 30 mA) equipped with a CCD 4k low-noise area detector. The detector-to-crystal working distance was 50 mm. A total of 1928 frames were collected in ϕ scan

Table 3. X-ray powder diffraction data for claraite. Intensities and d_{hkl} were calculated using the software *PowderCell* 2.3 (Kraus & Nolze, 1996) on the basis of the structural model given in Table 5. Only reflections with $I_{calc} \geq 10$ were reported, if not observed. Observed intensities were visually estimated (vs = very strong; s = strong; m = medium; mw = medium-weak; w = weak; vw = very weak).

I_{obs}	d_{obs}	Claraite Carrara (this work)			Claraite Clara mine Holotype material (this work)		Claraite Clara mine (Walenta & Dunn, 1982)	
		I_{calc}	d_{calc}	hkl	I_{obs}	d_{obs}	I_{obs}	d_{obs}
vs	13.6	100	13.59	0 0 1	vs	13.4	10	13.47
s	7.74	5	7.78	1 $\bar{1}$ 0	m	7.72	9	7.82
		13	7.76	1 1 0				
		2	7.69	$\bar{1}$ $\bar{1}$ 1				
vw	6.80	3	6.80	0 0 2	vw	6.76	1	6.83
vw	6.39	4	6.40	0 $\bar{2}$ 1	vw	6.34	–	–
mw	5.69	8	5.70	0 $\bar{2}$ 2	w	5.67	3	5.69
w	5.43	2	5.45	$\bar{1}$ $\bar{2}$ 1	w	5.42	0.5	5.51
		2	5.43	1 $\bar{2}$ 1				
m	5.15	4	5.17	2 0 0	m	5.15	6	5.17
		4	5.12	1 $\bar{2}$ 0				
		4	5.11	1 2 0				
vw	4.73	1	4.727	2 1 0	vw	4.71	–	–
vw	4.55	1	4.530	0 0 3	–	–	–	–
mw	4.34	3	4.338	$\bar{1}$ 2 1	w	4.34	3	4.37
		3	4.315	1 2 1				
mw	3.68	4	3.675	1 $\bar{3}$ 0	mw	3.66	8	3.65
		3	3.669	1 3 0				
m	3.632	9	3.626	0 $\bar{2}$ 4	m	3.621		
		1	3.603	2 1 2				
mw	3.402	3	3.398	0 0 4	w	3.394	3	3.42
mw	3.273	1	3.278	2 $\bar{3}$ 1	mw	3.267	5	3.24
		2	3.264	$\bar{2}$ $\bar{3}$ 2				
		1	3.262	$\bar{1}$ 3 1				
		1	3.250	1 3 1				
		1	3.245	2 $\bar{3}$ 2				
vw	3.128	1	3.125	1 $\bar{3}$ 4	vw	3.125	0.5	3.12
w	3.052	2	3.059	$\bar{2}$ 1 3	vw	3.055	–	–
		1	3.048	2 $\bar{3}$ 3				
–	–	1	3.023	2 1 3	vw	3.025	–	–
m	2.955	8	2.950	0 $\bar{2}$ 5	m	2.940	6	2.96
mw	2.841	3	2.850	0 $\bar{4}$ 4	w	2.850	3	2.84
		1	2.836	3 1 2				
w	2.807	1	2.819	1 3 2	w	2.798		–
		2	2.813	$\bar{1}$ $\bar{1}$ 5				
		3	2.792	1 $\bar{1}$ 5				
mw	2.720	1	2.726	$\bar{2}$ $\bar{4}$ 2	mw	2.724	4	2.72
		1	2.723	$\bar{1}$ $\bar{3}$ 5				
		3	2.718	0 0 5				
		2	2.717	2 $\bar{4}$ 2				

Table 3. (continued).

I_{obs}	d_{obs}	Claraite Carrara (this work)			Claraite Clara mine Holotype material (this work)		Claraite Clara mine (Walenta & Dunn, 1982)	
		I_{calc}	d_{calc}	hkl	I_{obs}	d_{obs}	I_{obs}	d_{obs}
		1	2.706	$1\bar{3}5$				
vw	2.648	2	2.643	$\bar{2}23$	vw	2.667	–	–
–	–	2	2.618	223	–	–	–	–
–	–	1	2.593	$3\bar{3}0$	–	–	–	–
–	–	2	2.586	330	–	–	–	–
		2	2.577	$\bar{2}\bar{2}5$				
		1	2.564	$0\bar{4}5$				
mw	2.563	1	2.562	$2\bar{4}0$	mw	2.570	3	2.57
		2	2.556	240				
		2	2.546	$2\bar{2}5$				
		2	2.505	$\bar{2}\bar{4}4$				
vw	2.492	2	2.486	$2\bar{4}4$	w	2.490	–	–
		1	2.438	$\bar{3}31$				
w	2.431	2	2.426	$\bar{4}02$	vw	2.421	0.5	2.42
		2	2.420	$\bar{2}05$				
		2	2.404	402				
w	2.406	2	2.392	205	–	–	–	–
		1	2.377	$\bar{2}41$				
		1	2.367	241				
w	2.366	1	2.366	$3\bar{3}4$	vw	2.383	–	–
		2	2.361	$\bar{4}\bar{2}2$				
–	–	2	2.345	$4\bar{2}2$	–	–	–	–
		2	2.297	$\bar{2}\bar{5}2$				
w	2.298	1	2.292	$2\bar{5}2$	mw	2.300	2	2.29
		2	2.272	$\bar{2}33$				
		1	2.258	$\bar{4}03$				
w	2.261	1	2.255	233	–	–	–	–
		2	2.240	$\bar{3}\bar{1}5$				
–	–	1	2.208	$3\bar{1}5$	–	–	–	–
vw	2.196	1	2.192	$\bar{3}\bar{3}5$	–	–	–	–
		1	2.137	$\bar{1}51$				
vw	2.138	1	2.133	151	vw	2.134	2	2.14
		1	2.123	$0\bar{6}2$				
w	2.039	1	2.035	510	–	–	–	–
vw	1.946	1	1.950	$\bar{2}\bar{5}6$	–	–	–	–
vw	1.892	1	1.886	$\bar{4}05$	–	–	–	–
vw	1.864	1	1.860	405	–	–	–	–
		1	1.794	$\bar{1}\bar{7}4$				
w	1.798	1	1.781	$1\bar{7}2$	mw	1.794	3	1.789
w	1.631	3	1.630	$0\bar{4}9$	mw	1.624	3	1.636

modes, in 0.5° slices. Exposure time was 45 s per frame. The data were integrated and corrected for Lorentz-polarization, background effects, and absorption, using the software package *Apex*2 (Bruker, AXS Inc., 2004),

Table 4. Crystal data and summary of parameters describing data collection and refinement for claraite.

Crystal data	
Structural formula	$(Cu,Zn)_{15}(AsO_4)_2(CO_3)_4(SO_4)(OH)_{14}\cdot 7H_2O$
Crystal size (mm)	$0.15 \times 0.05 \times 0.01$
Cell setting, space group	Triclinic, $P\overline{1}$
a, b, c (Å)	10.3343(6), 12.8212(7), 14.7889(9)
α, β, γ (°)	113.196(4), 90.811(4), 89.818(4)
V (Å^3)	1800.9(2)
Z	2
Data collection and refinement	
Radiation, wavelength (Å)	Mo$K\alpha$, $\lambda = 0.71073$
Temperature (K)	293
Maximum observed 2θ (°)	64.22
Measured reflections	29 556
Unique reflections	11 461
Reflections $F_o > 4\sigma(F_o)$	6956
R_{int} after absorption correction	0.0884
$R\sigma$	0.1393
Range of h, k, l	$-15 \leq h \leq 15$, $-19 \leq k \leq 17$, $-17 \leq l \leq 22$
R [$F_o > 4\sigma F_o$]	0.1110
R (all data)	0.1767
wR (on F_o^2)	0.3017
Goof	1.042
Number of least-squares parameters	363
Maximum and minimum residual peak (e/Å^3)	4.46 (at 1.65 Å from OH38) −3.44 (at 0.77 Å from Cu16)

resulting in a set of 11 461 independent reflections. The refined unit-cell parameters are $a = 10.3343(6)$ Å, $b = 12.8212(7)$ Å, $c = 14.7889(9)$ Å, $\alpha = 113.196(4)°$, $\beta = 90.811(4)°$, $\gamma = 89.818(4)°$, $V = 1800.9(2)$ Å^3. No obvious relationships between these unit-cell parameters and those given by Walenta (1999) could be found. The statistical tests on $|E|$ values ($|E^2 - 1| = 0.833$) suggested a centrosymmetric nature of claraite. Consequently, the crystal structure was solved in the space group $P\overline{1}$ using *SHELXS*-97 (Sheldrick, 2008).

After location of the metal positions, the crystal structure was completed through successive difference-Fourier maps. Scattering curves for neutral atoms were taken from the *International Tables for Crystallography* (Wilson, 1992). After several cycles of isotropic refinement using *SHELXL*-2014 (Sheldrick, 2015), the R_1 converged to 0.144. After introduction of the anisotropic displacement parameters for Cu, S, and As sites, the R_1 converged to 0.129. A check for possible twinning using the *PLATON* software (Spek, 2009) suggested the occurrence of a two-fold axis normal to (0 0 1). Notwithstanding a low twin ratio [0.94(1):0.06 (1)], the addition of the twin matrix improved the refinement that converged to $R_1 = 0.111$ for 6956 reflections with $F_o > 4\sigma(F_o)$ and 363 refined parameters. The anisotropic modeling of the displacement parameters of C and O positions resulted in several negatively defined values and did not significantly improved the refinement; consequently these atom positions were refined isotropically. Notwithstanding such a relatively high R value, the structure solution can be considered satisfactory as regards displacement parameters, atom coordinations, values of bond distances, as well as general crystal-chemical soundness. Details of data collection and refinement are given in Table 4.

3. Crystal structure description

3.1. General organization

Atomic coordinates and isotropic or equivalent isotropic displacement parameters of claraite are given in Table 5.

The crystal structure of claraite (Fig. 3) is formed by sixteen independent Cu sites, four C positions, two As sites, one S site, and forty-five anion positions in the asymmetric unit. It can be described as formed by {0 0 1} heteropolyhedral layers composed by $Cu\phi_5$ and $Cu\phi_6$ polyhedra as well as AsO_4 and CO_3 groups. Each layer can be described as built up by two symmetry-independent chain fragments of Cu-centered polyhedra connected along **a** through corner-sharing. The symmetry-independent chain fragments are attached along **b** through corner-sharing and through the occurrence of AsO_4 and CO_3 groups (Fig. 4a). The arsenate groups are bonded to the Cu-centered polyhedra through corner-sharing, whereas CO_3 groups are bonded through both corner-sharing and edge-sharing, the latter case being represented by the bonding between polyhedra centered by C3 and Cu9, and by C4 and Cu2.

The {0 0 1} heteropolyhedral layers are stacked along **c** through edge-sharing $Cu_2\phi_{10}$ and $Cu_2\phi_8$ dimers (Fig. 4b). The former is decorated by corner-sharing SO_4 groups, hosted within the channels occurring in the framework formed by the connection between the heteropolyhedral

Table 5. Atom fractional coordinates and isotropic or equivalent isotropic (∗) displacement parameters (Å^2) for claraite.

Site	x	y	z	U_{eq} (Å^2)
Cu1	½	0	½	0.0073(6)∗
Cu2	0.1341(2)	0.0991(2)	0.4395(2)	0.0062(4)∗
Cu3	0.2028(2)	0.6521(2)	0.2534(2)	0.0084(4)∗
Cu4	0.4785(2)	0.7294(2)	0.2794(2)	0.0094(5)∗
Cu5	0	½	½	0.0073(6)∗
Cu6	0.2867(2)	0.1544(2)	0.2522(2)	0.0086(4)∗
Cu7	0.0156(2)	0.2313(2)	0.2780(2)	0.0097(5)∗
Cu8	0.4990(2)	0.0236(2)	0.3057(2)	0.0068(4)∗
Cu9	0.6369(2)	0.4002(2)	0.5588(2)	0.0076(4)∗
Cu10	0.5206(2)	0.3178(2)	0.3134(2)	0.0098(5)∗
Cu11	0.9733(2)	0.8189(2)	0.3162(2)	0.0089(4)∗
Cu12	0.7865(2)	0.3928(2)	0.3466(2)	0.0090(4)∗
Cu13	0.9970(2)	0.5231(2)	0.3065(2)	0.0079(4)∗
Cu14	0.7092(2)	0.8926(2)	0.3462(2)	0.0077(4)∗
Cu15	0.9736(2)	0.5757(2)	0.1018(2)	0.0104(5)∗
Cu16	0.5015(4)	0.0665(3)	0.1042(2)	0.0326(9)∗
C1	0.755(2)	0.650(2)	0.236(2)	0.010(3)
C2	0.735(2)	0.151(2)	0.237(2)	0.013(4)
C3	0.754(2)	0.599(2)	0.646(2)	0.013(4)
C4	0.248(2)	0.900(2)	0.352(1)	0.007(3)
S	0.7111(5)	0.6774(5)	0.9971(4)	0.0153(10)∗
As1	0.3923(2)	0.2394(2)	0.4961(1)	0.0038(4)∗
As2	0.8916(2)	0.2602(2)	0.5026(1)	0.0037(4)∗
O1	0.6343(16)	0.6318(14)	0.2405(12)	0.019(3)
O2	0.8381(14)	0.5695(12)	0.1970(11)	0.011(3)
O3	0.8005(16)	0.7537(14)	0.2755(12)	0.018(3)
O4	0.6534(15)	0.0700(14)	0.2032(12)	0.017(3)
O5	0.6940(15)	0.2561(14)	0.2707(12)	0.017(3)
O6	0.8601(15)	0.1305(14)	0.2337(12)	0.018(3)
O7	0.8232(14)	0.5118(13)	0.6040(11)	0.013(3)
O8	0.1982(15)	0.3015(13)	0.3055(12)	0.016(3)
O9	0.3703(14)	0.4192(12)	0.3610(11)	0.012(3)
O10	0.3250(14)	0.9842(12)	0.3912(11)	0.013(3)
O11	0.1267(14)	0.9187(12)	0.3627(11)	0.011(3)
O12	0.2950(13)	0.7995(12)	0.3051(11)	0.010(3)
O13	0.673(2)	0.5643(17)	0.9870(16)	0.034(4)
O14	0.837(2)	0.705(2)	0.0460(18)	0.045(6)
O15	0.6160(19)	0.7618(17)	0.0527(16)	0.031(4)
O16	0.7242(18)	0.6804(16)	0.8969(14)	0.028(4)
O17	0.2308(13)	0.2431(12)	0.4974(10)	0.010(3)
O18	0.4498(13)	0.3716(11)	0.5535(10)	0.007(2)
O19	0.4442(15)	0.1864(12)	0.3787(10)	0.008(2)
O20	0.4468(12)	0.1600(11)	0.5594(10)	0.006(2)
O21	0.9475(14)	0.1305(12)	0.4482(11)	0.012(3)
O22	0.7308(13)	0.2532(13)	0.4991(11)	0.009(3)
O23	0.9443(13)	0.3383(11)	0.4389(10)	0.008(2)
O24	0.9487(12)	0.3146(11)	0.6221(10)	0.006(2)
OH25	0.6186(12)	0.0344(11)	0.4129(10)	0.006(2)
OH26	0.8665(12)	0.9249(11)	0.4246(10)	0.007(3)
OH27	0.1239(14)	0.1074(12)	0.2930(11)	0.012(3)
OH28	0.1107(14)	0.5095(12)	0.2021(12)	0.011(3)
OH29	0.3679(14)	0.6091(13)	0.2945(12)	0.014(3)
OH30	0.0599(12)	0.7125(11)	0.1989(10)	0.006(2)
OH31	0.5587(13)	0.8600(11)	0.2561(10)	0.008(2)
OH32	0.8798(13)	0.5344(12)	0.4119(10)	0.009(3)
OH33	0.3824(13)	0.0124(11)	0.1986(10)	0.008(2)
OH34	0.4257(13)	0.2138(12)	0.1964(10)	0.010(3)
OH35	0.9362(13)	0.3618(12)	0.2580(11)	0.010(3)
OH36	0.6298(12)	0.4253(11)	0.4234(10)	0.007(2)
OH37	0.8985(14)	0.4413(12)	0.9992(11)	0.012(3)
OH38	0.396(3)	0.050(2)	0.993(2)	0.058(7)
Ow39	0.415(2)	0.6518(19)	0.1090(17)	0.038(5)
Ow40	0.088(2)	0.164(2)	0.1136(18)	0.044(5)

Table 5. (continued).

Site	x	y	z	U_{eq} (Å^2)
Ow41	0.571(3)	0.418(3)	0.198(2)	0.061(7)
Ow42	0.910(2)	0.9134(19)	0.2081(17)	0.041(5)
Ow43	0.230(2)	0.8255(18)	0.1220(16)	0.035(4)
Ow44	0.833(3)	0.040(2)	0.004(2)	0.051(6)
Ow45	0.837(3)	0.297(3)	0.081(2)	0.069(8)

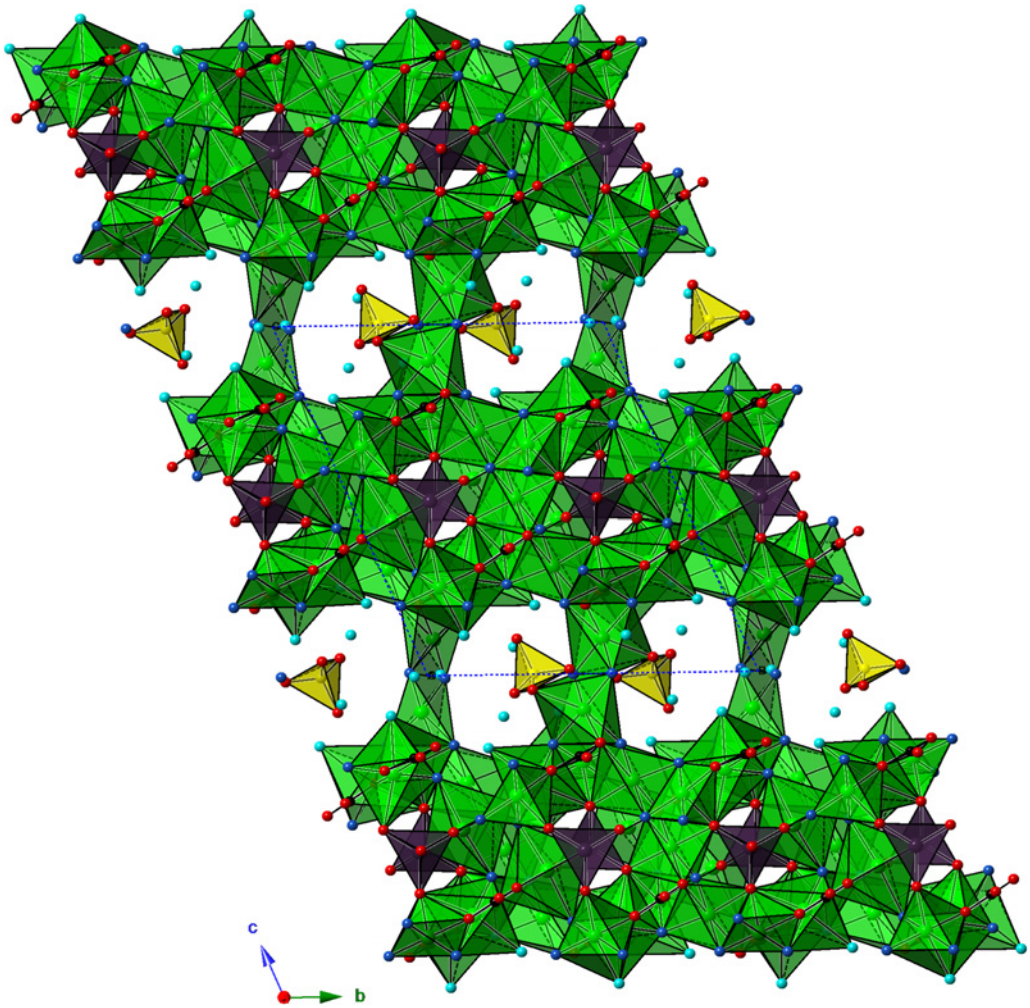

Fig. 3. Crystal structure of claraite as seen down [1 0 0]. Polyhedra: green = Cu sites; violet = As sites; black = C sites; yellow = S sites. Circles: red = O sites; blue = OH sites; light blue = H_2O sites. The unit cell is outlined.

layers and the dimers. In addition, the channels host H_2O groups. Following Eby & Hawthorne (1993), claraite can be classified as a compound having a framework structure.

Alternatively, the crystal structure can be described as formed by two kinds of {0 0 1} layers, *i.e.* an arsenate–carbonate-bearing layer alternating with a sulfate-bearing layer. The first one can be described as formed by (0 $\overline{2}$ 5) atomic layers (Fig. 5a) and forms electroneutral [$Cu_{13}(AsO_4)_2(CO_3)_4(OH)_{12}(H_2O)_4$] sheets. The chemical composition of the second layer (Fig. 5b) is [$Cu_2(SO_4)(OH)_2{\cdot}3H_2O$]; also this layer is electroneutral.

3.2. Atom coordinations

Table 6 reports selected bond distances and bond-valence sums (BVS) for cation positions, calculated according to the bond parameters given by Brese & O'Keeffe (1991).

In claraite, the sixteen independent Cu sites display five- to six-fold coordination. Usually they show the typically distorted (4+2) coordination (Fig. 6a) related to the Jahn–Teller effect of Cu^{2+} (*e.g.*, Burns & Hawthorne, 1996). Taking into account the nature of the ligands ϕ, the polyhedra types $CuO_4(OH)_2$ (Cu1 and Cu5 sites),

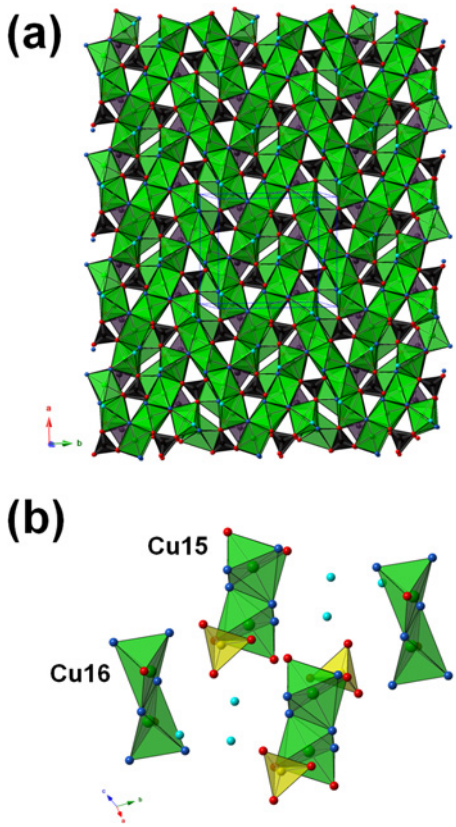

Fig. 4. The heteropolyhedral {0 0 1} layer (a) and the $Cu_2\phi_{8/10}$ dimers, decorated with SO_4 groups (b), connecting successive {0 0 1} layers. Same symbols as in Fig. 3.

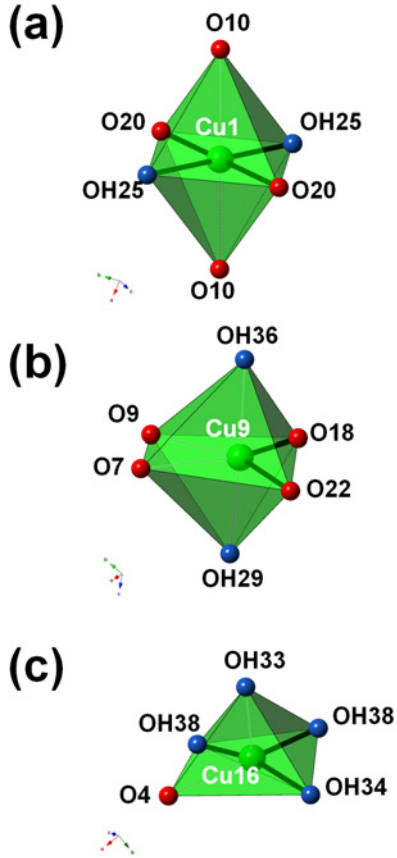

Fig. 6. Different kinds of (Cu,Zn) coordination polyhedra occurring in claraite. (a) A (4+2) distorted octahedron; (b) a (2+4) distorted octahedron; and (c) a square pyramidal polyhedron. Thick lines represent Cu–ϕ bond distances < ~2 Å, whereas dotted lines represent Cu–ϕ bond distances > ~2 Å.

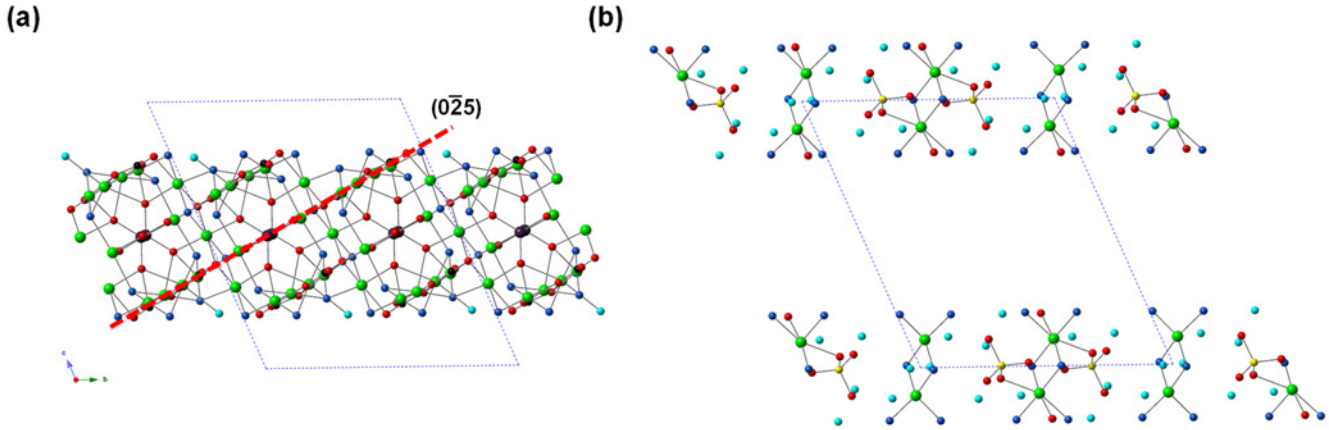

Fig. 5. Ball-and-stick representation of the crystal structure of claraite. (a) The arsenate–carbonate-bearing {0 0 1} layer; a (0 $\bar{2}$ 5) atomic layer is indicated by the dashed red line; (b) the sulfate-bearing layer. Symbols: green = Cu sites; violet = As sites; black = C sites; yellow = S sites; red = O sites; blue = OH sites; and light blue = H_2O sites.

$CuO_3(OH)_3$ (Cu8, Cu12, and Cu13), $CuO_3(OH)_2(H_2O)$ (Cu4, Cu7, Cu10, and Cu11), $CuO_2(OH)_4$ (Cu15), and $CuO_2(OH)_3(H_2O)$ (Cu3, Cu6, and Cu14) occur. The average of the four shorter Cu–ϕ distances, corresponding to the equatorial bonds, is 1.974 Å, with values ranging from 1.941 Å (Cu14) to 2.021 Å (Cu4), in agreement with the previous observations of Eby & Hawthorne (1993). The other two longer Cu distances, corresponding to the axial bonds, show a wider range of Cu–ϕ bond lengths, as a consequence of the weaker interaction at longer distances; in some cases, the sixth ligand is at a very long distance (Cu3, Cu6, Cu12, and Cu14), with Cu–ϕ

Table 6. Selected bond-distances (in Å) and bond-valence sums (BVS, in valence units, *v.u.*) for cation sites in claraite.

Cu1	–OH25	1.963(13) × 2	Cu2	–O21	1.964(14)	Cu3	–OH28	1.930(14)
	–O20	1.967(13) × 2		–O17	1.970(14)		–OH29	1.952(15)
	–O10	2.359(15) × 2		–O11	2.139(14)		–OH30	1.970(13)
	Mean	2.096		–OH26	2.149(13)		–O12	1.979(14)
	BVS	2.16		–OH27	2.212(15)		–O24	2.341(13)
				–O10	2.401(15)		Mean	2.034
				Mean	2.139		BVS	2.05
				BVS	1.87			
Cu4	–O1	1.984(17)	Cu5	–OH32	1.959(14) × 2	Cu6	–OH33	1.948(14)
	–OH29	2.006(15)		–O23	1.991(13) × 2		–O8	1.962(16)
	–OH31	2.022(13)		–O7	2.372(15) × 2		–OH34	1.965(14)
	–O12	2.071(14)		Mean	2.107		–OH27	1.969(14)
	–O20	2.362(14)		BVS	2.11		–O19	2.372(14)
	–Ow39	2.40(2)					Mean	2.043
	Mean	2.141					BVS	2.02
	BVS	1.90						
Cu7	–OH35	1.985(14)	Cu8	–OH33	1.936(14)	Cu9	–O18	1.964(13)
	–O6	1.999(16)		–OH25	1.958(13)		–O22	1.994(14)
	–OH27	2.021(14)		–O19	2.020(14)		–O9	2.148(15)
	–O8	2.058(16)		–OH31	2.026(14)		–OH36	2.150(13)
	–O23	2.358(14)		–O10	2.380(15)		–OH29	2.221(15)
	–Ow40	2.37(2)		–O4	2.446(16)		–O7	2.330(15)
	Mean	2.132		Mean	2.128		Mean	2.134
	BVS	1.93		BVS	2.04		BVS	1.85
Cu10	–O5	1.966(16)	Cu11	–O3	1.958(16)	Cu12	–O5	1.918(16)
	–OH34	1.968(14)		–OH30	1.960(14)		–OH36	1.939(13)
	–O9	1.973(15)		–O11	1.978(13)		–OH32	1.940(14)
	–OH36	2.003(14)		–OH26	1.991(14)		–OH35	1.978(14)
	–O19	2.390(13)		–O24	2.369(13)		–O23	2.387(14)
	–Ow41	2.56(3)		–Ow42	2.44(2)		Mean	2.032
	Mean	2.143		Mean	2.116		BVS	2.11
	BVS	2.03		BVS	2.10			
Cu13	–OH28	1.907(14)	Cu14	–O3	1.925(17)	Cu15	–OH37	1.947(15)
	–OH32	1.947(14)		–OH26	1.932(13)		–OH37	1.956(15)
	–OH35	2.003(14)		–OH25	1.938(13)		–OH30	1.981(13)
	–O24	2.004(13)		–OH31	1.968(14)		–O2	2.023(14)
	–O7	2.408(16)		–O20	2.411(13)		–OH28	2.418(14)
	–O2	2.520(15)		Mean	2.035		–O14	2.54(2)
	Mean	2.132		BVS	2.11		Mean	2.143
	BVS	2.10					BVS	2.03
Cu16	–OH38	1.90(3)	C1	–O1	1.27(2)	C2	–O4	1.28(3)
	–OH38	1.93(3)		–O2	1.29(2)		–O5	1.31(3)
	–OH34	2.008(14)		–O3	1.31(3)		–O6	1.31(3)
	–O4	2.119(16)		Mean	1.29		Mean	1.30
	–OH33	2.183(14)		BVS	3.90		BVS	3.83
	Mean	2.030						
	BVS	2.02						
C3	–O7	1.27(3)	C4	–O10	1.28(2)	S	–O13	1.45(2)
	–O8	1.29(3)		–O11	1.28(2)		–O14	1.46(3)
	–O9	1.30(2)		–O12	1.29(2)		–O15	1.46(2)
	Mean	1.29		Mean	1.28		–O16	1.51(2)
	BVS	3.98		BVS	4.01		Mean	1.47
							BVS	6.10
As1	–O17	1.669(14)	As2	–O21	1.644(15)			
	–O18	1.676(14)		–O22	1.664(14)			
	–O19	1.690(14)		–O23	1.717(13)			
	–O20	1.722(13)		–O24	1.720(14)			
	Mean	1.689		Mean	1.686			
	BVS	4.94		BVS	5.00			

Table 7. Bond-valence sums (in valence units, *v.u.*) for anion positions in claraite.

Site	*v.u.*	Site	*v.u.*	Site	*v.u.*
O1	1.81	O16	1.38	OH31	1.25
O2	1.79	O17	1.76	OH32	1.45
O3	2.22	O18	1.74	OH33	1.24
O4	1.79	O19	1.93	OH34	1.33
O5	2.22	O20	1.88	OH35	1.30
O6	1.65	O21	1.86	OH36	1.19
O7	1.86	O22	1.75	OH37	0.96
O8	2.13	O23	1.88	OH38	1.05
O9	2.01	O24	1.87	Ow39	0.14
O10	1.81	OH25	1.43	Ow40	0.15
O11	2.08	OH26	1.22	Ow41	0.09
O12	2.09	OH27	1.09	Ow42	0.13
O13	1.59	OH28	1.18	Ow43	0.00
O14	1.57	OH29	1.12	Ow44	0.00
O15	1.56	OH30	1.37	Ow45	0.00

Table 8. O···O distances, corresponding bond strengths (in valence units, *v.u.*), and corrected bond-valence sums for hydrogen-bond contributions at anion sites.

O···O donor → acceptor	*d* (Å)	*v.u.*	O···O donor → acceptor	*d* (Å)	*v.u.*
OH25 → O22	2.83(2)	0.17	Ow39 → O15	2.82(3)	0.18
OH26 → O21	2.66(2)	0.25	Ow40 → O16	2.83(3)	0.17
OH27 → Ow42	3.18(3)	0.10	Ow40 → Ow44	3.16(4)	0.11
OH28 → O16	2.87(2)	0.16	Ow41 → O1	2.65(3)	0.25
OH29 → Ow41	3.12(3)	0.11	Ow41 → Ow45	3.31(4)	0.09
OH30 → Ow43	2.80(2)	0.18	Ow42 → O6	2.71(3)	0.22
OH31 → O15	2.84(2)	0.17	Ow42 → O14	2.89(3)	0.16
OH32 → O17	2.87(2)	0.15	Ow43 → Ow39	2.88(3)	0.16
OH33 → Ow43	2.71(2)	0.22	Ow43 → Ow44	3.06(3)	0.12
OH34 → O16	2.75(2)	0.20	Ow43 → Ow45	2.86(4)	0.16
OH35 → Ow45	2.61(4)	0.28	Ow44 → OH38	2.65(4)	0.25
OH36 → O18	2.62(2)	0.27	Ow44 → Ow40	2.64(4)	0.26
OH37 → O13	2.85(2)	0.17	Ow45 → OH37	2.65(3)	0.25
OH38 → O15	2.75(3)	0.20	Ow45 → Ow44	3.04(4)	0.12
Ow39 → O13	2.72(3)	0.22			

Site	BVS	Species	Site	BVS	Species	Site	BVS	Species
O1	2.06	O	O16	1.91	O	OH31	1.08	OH
O2	1.79	O	O17	1.91	O	OH32	1.30	OH
O3	2.22	O	O18	2.01	O	OH33	1.02	OH
O4	1.79	O	O19	1.93	O	OH34	1.13	OH
O5	2.22	O	O20	1.88	O	OH35	1.02	OH
O6	1.87	O	O21	2.11	O	OH36	0.92	OH
O7	1.86	O	O22	1.92	O	OH37	1.04	OH
O8	2.13	O	O23	1.88	O	OH38	1.10	OH
O9	2.01	O	O24	1.87	O	Ow39	−0.10	H_2O
O10	1.81	O	OH25	1.26	OH	Ow40	0.11	H_2O
O11	2.08	O	OH26	0.97	OH	Ow41	−0.14	H_2O
O12	2.09	O	OH27	0.99	OH	Ow42	−0.15	H_2O
O13	1.98	O	OH28	1.02	OH	Ow43	−0.04	H_2O
O14	1.73	O	OH29	1.01	OH	Ow44	−0.16	H_2O
O15	2.11	O	OH30	1.19	OH	Ow45	0.16	H_2O

distances ranging from 2.91(2) Å (Cu6–Ow40) to 3.20 (2) Å (Cu12–O6). In these cases, the coordination polyhedron of Cu^{2+} could be more properly described as a square pyramid, in particular for the Cu12 site.

The six-coordinated Cu2 and Cu9 sites show two bond lengths definitely shorter than the other four ones (*i.e.* 1.96–1.99 Å *vs.* 2.14–2.40 Å). Interestingly, this (2+4) bond configuration (Fig. 6b) is not another kind of Jahn–

Table 9. Copper secondary minerals characterized by the occurrence of mixed AsO_4, CO_3, and SO_4 groups.

Mineral	Chemical formula	*a* (Å)	*b* (Å)	*c* (Å)	α (°)	β (°)	γ (°)	S.G.	Ref.
Mixed AsO_4–SO_4									
Arsentsumebite	$CuPb_2(AsO_4)(SO_4)(OH)$	7.80	5.89	8.96	90	112.3	90	$P2_1/m$	[1]
Barrotite	$Cu_9Al(HSiO_4)_2[(SO_4)(HAsO_4)_{0.5}](OH)_{12}\cdot 8H_2O$	10.65	10.65	21.95	90	90	120	$P3_1$ or $P3_2$	[2]
Chalcophyllite	$Cu_{18}Al_2(SO_4)_4(SO_4)_3(OH)_{24}\cdot 36H_2O$	10.76	10.76	28.68	90	90	120	$R\overline{3}$	[3]
Leogangite	$Cu_{10}(AsO_4)_4(SO_4)(OH)_6\cdot 8H_2O$	21.77	12.33	10.72	90	92.8	90	$C2/c$	[4]
Parnauite	$Cu_9(AsO_4)_2(SO_4)(OH)_{10}\cdot 7H_2O$	3.01	14.26	14.93	90	90	90	$Pmn2_1$	[5]
Tangdanite	$Ca_2Cu_9(AsO_4)_4(SO_4)_{0.5}(OH)_9\cdot 9H_2O$	54.49	5.57	10.47	90	96.3	90	$C2/c$	[6]
Unnamed mineral	$Cu_{10}(AsO_4)_4(SO_4)(OH)_6\cdot 12H_2O$	10.76	12.29	12.13	90	92.9	90	$P2_1$	[7]
Vasilseverginite	$Cu_9O_4(AsO_4)_2(SO_4)_2$	8.11	9.92	11.02	90	110.9	90	$P2_1/n$	[8]
Mixed AsO_4–CO_3									
Tyrolite-1*M*	$Ca_2Cu_9(AsO_4)_4(CO_3)(OH)_8\cdot 11H_2O$	27.56	5.57	10.47	90	98.1	90	$P2/c$	[9]
Tyrolite-2*M*	$Ca_2Cu_9(AsO_4)_4(CO_3)(OH)_8\cdot 11H_2O$	54.52	5.56	10.46	90	96.4	90	$C2/c$	[9]
Mixed CO_3–SO_4									
Caledonite	$Cu_2Pb_5(SO_4)_3(CO_3)(OH)_6$	20.08	7.14	6.56	90	90	90	$Pmn2_1$	[10]
Nakauriite	$Cu_8(SO_4)_4(CO_3)(OH)_6\cdot 48H_2O$	14.58	11.47	16.22	90	90	90	unknown	[11]
Mixed AsO_4–CO_3–SO_4									
Claraite	$(Cu,Zn)_{15}(AsO_4)_2(CO_3)_4(SO_4)(OH)_{14}\cdot 7H_2O$	10.33	12.82	14.79	113.2	90.8	89.8	$P\overline{1}$	[12]

[1] Zubkova *et al.* (2002); [2] Sarp *et al.* (2014); [3] Sabelli (1980); [4] Lengauer *et al.* (2004); [5] Mills *et al.* (2013); [6] Ma *et al.* (2014); [7] Kolitsch & Lengauer (2014); [8] Pekov *et al.* (2015); [9] Krivovichev *et al.* (2006); [10] Schofield *et al.* (2009); [11] Suzuki *et al.* (1976); [12] this work.

Teller distortion, but it is actually related to the displacement of the Cu atom in the opposite direction with respect to the edge shared with CO_3 groups.

Finally, Cu16 shows a square pyramidal coordination (Fig. 6c). This polyhedron shares an edge with another symmetry-related Cu16ϕ_5 pyramid to form a $Cu_2\phi_8$ dimer (*e.g.*, Eby & Hawthorne, 1993).

As reported above, chemical data point to the occurrence of ~13 Cu and ~2 Zn apfu. Owing to the similar scattering factors of Cu ($Z=29$) and Zn ($Z=30$) and their similar ionic radius (0.73 and 0.74 Å for six-fold coordinated Cu^{2+} and Zn^{2+}, respectively; Shannon, 1976), the positioning of these two elements in the claraite structure can be hypothesized on the basis of the geometrical features of the cation-centered polyhedra only. As observed in other (Cu,Zn) phases (*e.g.*, ktenasite – Mellini & Merlino, 1978; rosasite – Perchiazzi, 2006; aurichalcite – Giester & Rieck, 2014), the polyhedra hosting Zn are more regular, even if a slight distortion can be observed resulting from a partial Cu occupancy. In agreement with Mellini & Merlino (1978), the degree of distortion of the Cu polyhedra of claraite could be evaluated taking into account the difference Δl between the average values of axial and equatorial bond distances. In such a way, the Δl values of the Cu sites showing the Jahn–Teller effect range between ~0.35 and ~0.50 Å, the lowest values being observed at Cu4 and Cu7 sites. Moreover, small values of Δl have been observed at the Cu2 and Cu9 sites (0.06 and 0.08 Å, respectively). On the basis of the above considerations, it is reasonable to assume that zinc could be preferentially hosted at the Cu2 and Cu9 sites; additionally, minor replacements of Cu by Zn could occur also at the Cu4 and Cu7 positions.

The four independent C positions in claraite show the typical triangular planar coordination, with ⟨C–O⟩ distances ranging between 1.27 and 1.31 Å, and O–C–O angles between 115(2)° and 123(2)°. The crystal structure is completed by two As and one S sites. Both arsenic and sulfur are tetrahedrally coordinated, with average ⟨As–O⟩ and ⟨S–O⟩ distances of 1.688 and 1.47 Å, respectively, in good agreement with literature values (*e.g.*, Hawthorne *et al.*, 2000; Majzlan *et al.*, 2014).

The forty-five independent anion positions can be divided, on the basis of their BVS (Table 7), in O^{2-}, OH^-, and H_2O-hosting sites. Indeed, BVS range from 0.00 valence unit (*v.u.*) to 2.22 *v.u.* Several sites have BVS around 1 *v.u.*, probably representing OH^- groups. Anion coordination ranges from one (atoms linked at the corners of Cu or S polyhedra) to four, being bonded to three Cu sites and one C or As site. Two- and three-fold coordinations occur as well. Some anion positions are hosted within the [1 0 0] channels and are occupied by H_2O groups.

3.3. Hydrogen bonds in claraite

The occurrence of several underbonded oxygen atoms, as well as the examination of short O···O distances, allowed to hypothesize the occurrence of a complex hydrogen-bond system, even if hydrogen atoms were not located owing to the low diffraction quality of the available material. The observed O···O distances agree with those calculated on the basis of Raman spectroscopy, suggesting the occurrence of O···O distances of ~2.7, ~2.8, and ~3.0 Å. Table 8 gives short O···O distances and the corresponding bond strength calculated in agreement with Ferraris & Ivaldi (1988). The species occurring at the

different anion positions are reported, indicating the presence of $24O^{2-}$, $14OH^{-}$, and $7H_2O$ groups in the crystal structure of claraite. Notwithstanding the relatively low quality of the structural refinement, the BVS at the anion positions are satisfying. Oxygen atoms display BVS ranging from 1.73 to 2.22 *v.u.*, hydroxyl groups have BVS between 0.92 and 1.30 *v.u.*, whereas H_2O groups have BVS in the range −0.16 to 0.16 *v.u.*

4. Discussion

The collection of new chemical and crystallographic data on two specimens of claraite from the type locality and from Carrara confirmed the occurrence of As and S, as reported by other authors (*e.g.*, Schnorrer, 2000; Kolitsch & Brandstätter, 2012; Putz *et al.*, 2012). In addition, the solution of the crystal structure allowed to clarify the crystal-chemical role of these two elements. Thus, claraite has been redefined as a mixed-anion mineral containing $(AsO_4)^{3-}$, $(CO_3)^{2-}$, $(SO_4)^{2-}$, as well as $(OH)^{-}$ and H_2O groups. Its ideal chemical formula is $(Cu,Zn)_{15}(AsO_4)_2(CO_3)_4(SO_4)(OH)_{14}\cdot 7H_2O$.

Among Cu oxysalts, there are some mixed-anion minerals, showing the coexistence of AsO_4 and SO_4, AsO_4 and CO_3, and SO_4 and CO_3 groups (Table 9). However, claraite is the only known mineral showing the simultaneous presence of AsO_4, CO_3, and SO_4 groups and it could be the result of the alteration of Cu–As sulfide minerals in a $(HCO_3)^{-}$-rich environment, like that represented by the marble cavities of Carrara, where some Cu–As sulfides occur (*e.g.*, enargite and its dimorph luzonite).

Acknowledgments: Vittorio Mattioli and Riccardo Mazzanti are thanked for providing us with the studied specimens. The holotype material was kindly provided by the Smithsonian Institution – National Museum of Natural History, Washington, DC, USA. Stefano Merlino is acknowledged for useful discussion and for the critical reading of the manuscript; Simona Bigi is thanked for electron microprobe analysis. The comments of Taras L. Panikorovskii and Uwe Kolitsch have been greatly appreciated, helping us to improve the paper.

References

Brese, N.E. & O'Keeffe, M. (1991): Bond-valence parameters for solids. *Acta Crystallogr.*, **B47**, 192–197.

Bruker, AXS Inc. (2004): APEX 2. Bruker Advanced X-ray Solutions, Madison, WI, USA.

Burns, P.C. & Hawthorne, F.C. (1996): Static and dynamic Jahn–Teller effects in Cu^{2+} oxysalt minerals. *Can. Mineral.*, **34**, 1089–1105.

Eby, R.K. & Hawthorne, F.C. (1993): Structural relations in copper oxysalt minerals. I. Structural hierarchy. *Acta Crystallogr.*, **B49**, 28–56.

Ferraris, G. & Ivaldi, G. (1988): Bond valence *vs* bond length in O···O hydrogen bonds. *Acta Crystallogr.*, **B44**, 341–344.

Frost, R.L. & Kloprogge, J.T. (2003): Raman spectroscopy of some complex arsenate minerals – implications for soil remediation. *Spectrochim. Acta*, **A59**, 2797–2804.

Frost, R.L., Williams, P.A., Kloprogge, J.T. (2003): Raman spectroscopy of lead sulphate–carbonate minerals – implications for hydrogen bonding. *N. Jb. Mineral. Monat.*, **2003**, 529–542.

Frost, R.L., Sejkora, J., Čejka, J., Keeffe, E.C. (2009): Raman spectroscopic study of the mixed anion sulphate–arsenate mineral parnauite $Cu_9[(OH)_{10}|SO_4|(AsO_4)_2]\cdot 7H_2O$. *J. Raman Spectrosc.*, **40**, 1546–1550.

Giester, G. & Rieck, B. (2014): Crystal structure refinement of aurichalcite, $(Cu,Zn)_5(CO_3)_2(OH)_6$, from the Lavrion Mining District, Greece. *N. Jb. Miner. Abh. (J. Min. Geochem.)*, **191**, 225–232.

Hawthorne, F.C., Krivovichev, S.V., Burns, P.C. (2000): The crystal chemistry of sulfate minerals. *Rev. Mineral. Geochem.*, **40**, 1–112.

Kolitsch, U. & Brandstätter, F. (2012): 1743) Baryt, Chalkophyllit und Clarait vom Pengelstein bei Kitzbühel, Tirol. *in* "Neue Mineralfunde aus Österreich LXI", G. Niedermayr, C. Auer, F. Bernhard, H.-P. Bojar, F. Brandstätter, M. Habel, C.E. Hollerer, G. Knobloch, U. Kolitsch, B. Kutil, E. Löffler, K. Mörtl, R. Poeverlein, W. Postl, H. Prasnik, A. Prayer, H. Pristacz, T. Schachinger, C. Steinwender, J. Taucher, A. Thinschmidt, F. Walter, eds. *Carinthia II*, **202/122**, 123–180.

Kolitsch, U. & Lengauer, C.L. (2014): Crystal structure of $Cu_{10}(AsO_4)_4(SO_4)(OH)_6\cdot 12H_2O$, a new copper arsenate–sulphate mineral closely related to leogangite. *in* "92nd Annual Meeting of the DMG, Jena, Germany, September 21–24; Programme Abstracts", 258.

Kraus, W. & Nolze, G. (1996): PowderCell – a program for the representation and manipulation of crystal structures and calculation of the resulting X-ray powder patterns. *J. Appl. Crystallogr.*, **29**, 301–303.

Krivovichev, S.V., Chernyshov, D.Y., Döbelin, N., Armbruster, T., Kahlenberg, V., Kaindl, R., Ferraris, G., Tessadri, R., Kaltenhauser, G. (2006): Crystal chemistry and polytypism of tyrolite. *Am. Mineral.*, **91**, 1378–1384.

Lengauer, C.L., Giester, G., Kirchner, E. (2004): Leogangite, $Cu_{10}(AsO_4)_4(SO_4)(OH)_6\cdot 8H_2O$, a new mineral from the Leogang mining district, Salzburg province, Austria. *Mineral. Petrol.*, **81**, 187–201.

Libowitzky, E. (1999): Correlation of O–H stretching frequencies and O–H···O hydrogen bond lengths in minerals. *Monat. Chem.*, **130**, 1047–1059.

Ma, Z., Li, G., Chukanov, N.V., Poirier, G., Shi, N. (2014): Tangdanite, a new mineral species from the Yunnan Province, China and the discreditation of 'clinotyrolite'. *Mineral. Mag.*, **78**, 559–569.

Majzlan, J., Drahota, P., Filippi, M. (2014): Parageneses and crystal chemistry of arsenic minerals. *Rev. Mineral. Geochem.*, **79**, 17–184.

Mellini, M. & Merlino, S. (1978): Ktenasite, another mineral with ${}^{2}_{\infty}[(Cu,Zn)_2(OH)_3O]^{-}$ octahedral sheets. *Z. Kristallogr.*, **147**, 129–140.

Mills, S.J., Kampf, A.R., McDonald, A.M., Bindi, L., Christy, A.G., Kolitsch, U., Favreau, G. (2013): The crystal structure of parnauite: a copper arsenate–sulphate with translational disorder of structural rods. *Eur. J. Mineral.*, **25**, 693–704.

Orlandi, P. (1999): Zibaldone di mineralogia italiana 1999. *Riv. Mineral. Ital.*, **23**, 170–175.

Pekov, I.V., Britvin, S.N., Yapaskurt, V.O., Krivovichev, S.V., Vigasina, M.F., Sidorov, E.G. (2015): Vasilseverginite, IMA 2015-083. CNMNC Newsletter No. 28, December 2015, page 1864. *Mineral. Mag.*, **79**, 1859–1864.

Perchiazzi, N. (2006): Crystal structure determination and Rietveld refinement of rosasite and mcguinnessite. *Z. Kristallogr.*, **23**, 505–510.

Putz, H., Lechner, A., Poeverlein, R. (2012): Erythrin und Clarait vom Pichlerstollen am Silberberg bei Rattenberg, Nordtirol. *Lapis*, **37**, 37–52, 62.

Sabelli, C. (1980): The crystal structure of chalcophyllite. *Z. Kristallogr.*, **151**, 129–140.

Sarp, H., Černý, R., Pushcharovsky, D.Y., Schouwink, P., Teyssier, J., Williams, P.A., Babalik, H., Mari, G. (2014): La barrotite, $Cu_9Al(HSiO_4)_2[(SO_4)(HAsO_4)_{0.5}](OH)_{12}\cdot 8H_2O$, un nouveau minéral de la mine de Roua (Alpes-Maritimes, France). *Riv. Sci.*, **98**, 3–22.

Schnorrer, G. (2000): Mineralogische Notizen VII. *Der Aufschluss*, **51**, 281–293.

Schofield, P.F., Wilson, C.C., Knight, K.S., Kirk, C.A. (2009): Proton location and hydrogen bonding in the hydrous lead copper sulfates linarite, $PbCu(SO_4)(OH)_2$, and caledonite, $Pb_5Cu_2(SO_4)_3CO_3(OH)_6$. *Can. Mineral.*, **47**, 649–662.

Shannon, R.D. (1976): Revised effective ionic radii and systematic studies of interatomic distances in halides and chalcogenides. *Acta Crystallogr.*, **A32**, 751–767.

Sheldrick, G.M. (2008): A short history of SHELX. *Acta Crystallogr.*, **A64**, 112–122.

— (2015): Crystal structure refinement with *SHELXL*. *Acta Crystallogr.*, **C71**, 3–8.

Spek, A.L. (2009): Structure validation in chemical crystallography. *Acta Crystallogr.*, **D65**, 148–155.

Suzuki, J., Ito, M., Sugiura, T. (1976): A new copper sulfate–carbonate hydroxide hydrate mineral, $(Mn,Ni,Cu)_8(SO_4)_4(CO_3)(OH)_6\cdot 48H_2O$, from Nakauri, Aichi Prefecture, Japan. *J. Mineral. Petrol. Econ. Geol.*, **71**, 183–192.

Walenta, K. (1999): On the lattice constants of claraite. *Der Erzgräber*, **13**, 20–22 (in German).

Walenta, K. & Dunn, P.J. (1982): Clarait, ein neues Karbonatmineral aus der Grube Clara (mittlerer Schwarzwald). *Chem. Erde*, **41**, 97–102.

Wilson, A.J.C., ed. (1992): International Tables for X-ray Crystallography, Volume C: Mathematical, Physical and Chemical Tables. Kluwer Academic, Dordrecht, Netherlands.

Wojdyr, M. (2010): *Fityk*: a general-purpose peak fitting program. *J. Appl. Crystallogr.*, **43**, 1126–1128.

Zubkova, N.V., Pushcharovsky, D.Y., Giester, G., Tillmanns, E., Pekov, I.V., Kleimenov, D.A. (2002): The crystal structure of arsentsumebite, $Pb_2Cu[(As,S)O_4]_2(OH)$. *Mineral. Petrol.*, **75**, 79–88.

Received 30 March 2017
Modified version received 25 May 2017
Accepted 8 June 2017